Reversible and High-Capacity Data Hiding in High Quality Medical Images

Li-Chin Huang[3], Min-Shiang Hwang[1] and Lin-Yu Tseng[2]
[1] Department of Computer Science & Information Engineering Asia University
Taichung 41354, Taiwan
[e-mail: mshwang@asia.edu.tw]
[2] Department of Computer Science and Communication Engineering, Providence University
Taichung 43301, Taiwan
[e-mail: lytseng@pu.edu.tw]
[3] Department of Computer Science and Engineering, National Chung Hsing University
Taichung 402, Taiwan
[e-mail: phd9406@cs.nchu.edu.tw]

*Corresponding author: Min-Shiang Hwang

Received September 21, 2012; revised November 22, 2012; accepted December 21, 2012; published January 29, 2013

Abstract

Via the Internet, the information infrastructure of modern health care has already established medical information systems to share electronic health records among patients and health care providers. Data hiding plays an important role to protect medical images. Because modern medical devices have improved, high resolutions of medical images are provided to detect early diseases. The high quality medical images are used to recognize complicated anatomical structures such as soft tissues, muscles, and internal organs to support diagnosis of diseases. For instance, 16-bit depth medical images will provide 65,536 discrete levels to show more details of anatomical structures. In general, the feature of low utilization rate of intensity in 16-bit depth will be utilized to handle overflow/underflow problem. Nowadays, most of data hiding algorithms are still experimenting on 8-bit depth medical images. We proposed a novel reversible data hiding scheme testing on 16-bit depth CT and MRI medical image. And the peak point and zero point of a histogram are applied to embed secret message k bits without salt-and-pepper.

Keywords: reversible data embedding, histogram, peak point, zero point, medical image

http://dx.doi.org/10.3837/tiis.2013.01.009

1. Introduction

Based on digital information management, the information infrastructure of modern health care has already established the medical information systems to share certified electronic health records of individual patients (such as personal stats, medical history, and radiology images) among patients, medical professionals, health care providers, and health care organizations via the Internet. However, the illegal attackers are more and more increasing to get information via the Internet through interception, unauthorized tampering, and illegal accessing. Data hiding is one of feasible methodologies to protect medical images in authentication, fingerprinting, copy control, security, covert communication.

According to permanent distortion of the cover images, there are two classes of data hiding schemes: fragile and robust (semi-fragile) [20][21][26]. Because the cover image is distorted permanently, the original image is unable to restore from a stego image. Therefore, these kinds of schemes cannot satisfy certain fields such as medical imaging systems, artwork preserving, military imaging systems, remote sensing systems, high precision systems in scientific research, and the field of law enforcement.

Reversible data hiding schemes, also called as lossless data embedding, can restore the original image from stego images blindly after the hidden data was retrieved. Nowadays, reversible data hiding schemes have been proposed by researchers [20][25][34][35]. In general, data hiding techniques are divided into four main kinds of techniques: data compression [1][7][33], pixel-value difference expansion (DE) scheme [20][34], cryptography base scheme [5][6][29][33] and histogram scheme [9][12][16].

Recently, some researches [2][12][33] pay attention to data compression based on reversible data because the digital images in compressed format conceal secret data, shorten transmission time on the Internet, and take up less storage space. In general, the data compression based on reversible data hiding schemes are developed for images compressed by JPEG [3], vector quantization [7][18], block truncation coding [4].

DE scheme is proposed by Tian [28] by examining the redundancy between the two neighboring pixels to realize a high capacity and low distortion data hiding. Kim et al. [13] develop the DE method to reduce the location map. After processing pixel values, Tina's scheme will cause the double expansion of the pixel values. Thus, the gray values which are greater than 255 in 8-bit depth will be abandoned to prevent the reduction of the image quality. In order to improve this drawback and increase capacity, Lou et al. [15] developed a reduction DE method to adjust the expansion difference and embedding data into multiple layers in medical images.

Vleeschouwer et al. [30] proposed a circular interpretation of bijective transformation data hiding with histogram shifting techniques. Ni et al. [20] applies a zero point and peak point of an image histogram to hide secret bits. Fallahpour et al. [9] adopts number of pairs (peak, zero) points based on the histogram shifting to embed the data. Based on a histogram, Weng et al. [34] present a prediction-based reversible data hiding.

Cryptography base scheme [6] regards steganography as cryptography. Therefore, a variety of secret communications messages can be embedded in a stego-image and even appear invisible. Many cryptography methods are applied to data hiding such as Elliptic Curve Cryptography (ECC) and secret sharing schemes. In 2012, Vigila et al. [29] developed an ECC based data hiding method. It would advantage ECC cryptography to develop systems in smart cards, a mobile phone and other tiny devices because of a smaller key size, faster computation,

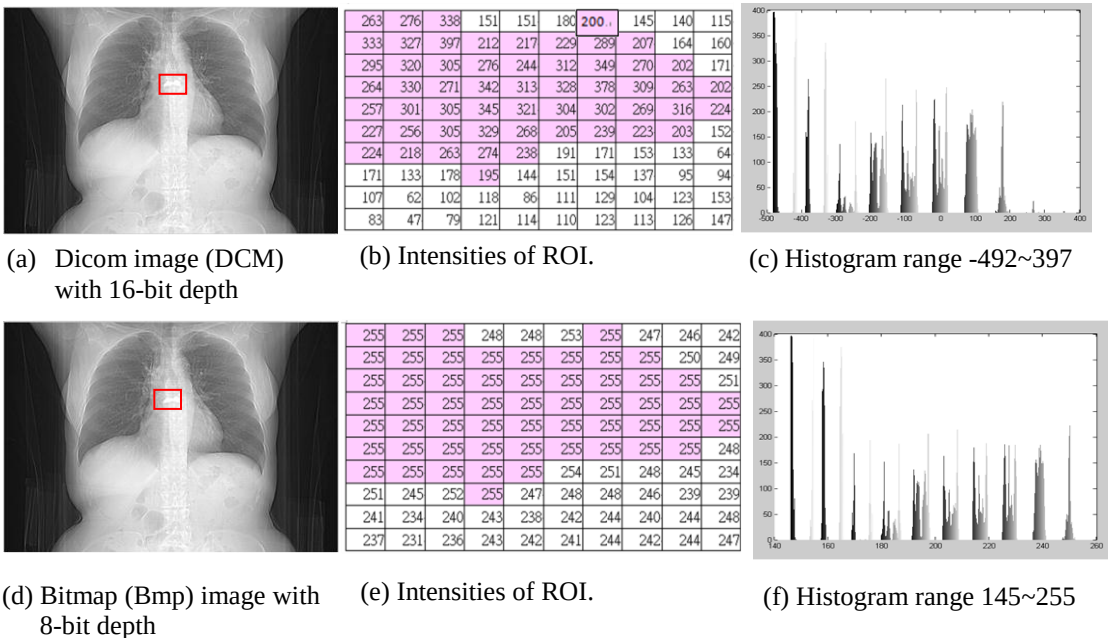

(a) Dicom image (DCM) with 16-bit depth

(b) Intensities of ROI.

(c) Histogram range -492~397

(d) Bitmap (Bmp) image with 8-bit depth

(e) Intensities of ROI.

(f) Histogram range 145~255

Fig.1. 16-bit depth dicom image compared with 8-bit depth bitmap image

reduced power consumption, and less storage requirements. Most of secret sharing data hiding schemes are based on Shamir's secret sharing theory. In general, secret sharing schemes split a secret data into several pieces assigned to a group of people and keep a secret share independently. Recently, Wu et al. [5] proposed a sharing scheme based on data hiding method by applying an optimal pixel adjustment process to enhance the image quality.

Data hiding is an important technique to apply medical images. In 2011, Chang et al. [8] utilizes repetitive pixels to hide secret messages in medical image without the location map compression. Without the restoration of the original medical images, the stego images are still able to provide some preliminary diagnosis for health care providers. Therefore, some data hiding schemes [8][9] embedded secret bits into the Region of Non-Interest (RONI) and less secret bits were embedded into the Region of None Interest (ROI). In mobile healthcare applications, Rochan et al. [24] combines an arithmetic coding with cryptography to embed data in medical images. During diagnosis and treatment, Fallahpour et al. [9] proposed the requirement of gradual medical data insertion b doctor observations.

A 8-bit depth medical image will demonstrate the image intensity from 0 to 255. However, the high resolution medical images (ex: 16-bit depth) are required to improve the detection rate of diseases so treat at the early stage. And the medical devices (i.g., CT scanner) are more and more precise to present complicated anatomical structures in images. The high quality medical images with 16-bit depth utilize intensity 65,536 discrete levels demonstrate more details of the smooth surface of anatomical structures. More intensity discrete levels may reduce duplicate intensity. In other words, duplicated intensity is more common in 8-bit depth medical images than in 16-bit depth medical images. For instance, a white area of lung medical image is expressed by 255 in 8-bit depth image and expressed by different intensity values in 16-bit depth image shown in **Fig. 1** Let image utilization rate of intensity is (max intensity value – min intensity value) $/ 2^{bit\ depth}$. In general, 16-bit depth images have low

utilization rate of intensity. On the contrary, 8-bit depth images have high utilization rate of intensity. Because of 16-bit depth images have low utilization rate, more intensities will be required to handle the overflow or underflow problems. However, 8-bit depth images have less intensity to handle the overflow/underflow problems. The comparison of 16-bit and 8-bit depth medical images is shown in **Table 1**.

Nowadays, most of data hiding schemes [8][9][15][20][21][27] were tested on 8-bit depth medical images. Overflow/underflow problems in 8-bit depth images are more serious than in 16-bit depth images. Most of schemes adopted the location map with compression techniques or modulo-256 addition to handle overflow/underflow problems. Nevertheless, the method of a location map will consume capacities for embedding to an image [1][16]. And the method of modulo-256 addition often suffers from the annoying salt-and-pepper noise [17].

Ni. et al. [20] developed one zero point and one peak point shifting histogram by embedding secret messages. Furthermore, they also proposed multiple pairs of Maximum and Minimum points to hide secret bits. In 2011, Fallahpour et al. [9] utilized number pairs of histograms (zeros, peaks) to relocate and embed secret data. We propose multi-levels schemes by number pairs of histograms (zeros, peaks) to embed k bits secret data, and compute the histogram central rate to handle overflow/underflow problems testing on 16-bit depth dicom format medical images.

This paper is organized as follows: Section 2 describes our method. Section 3 presents the experimental results. And conclusions are drawn in section 4.

2. Proposed Method

In this paper, we apply number of pairs (peak, zero) points in image intensity histograms to embed n bits secret messages for each block. We also adopt centralized utilization rate to handle overflow/underflow problems. The histogram for different kinds of medical images, Lung CT (512×512 pixels) and Brain MRI (256×256) with 16-bit depth dcm format is shown in **Fig. 2**. The peak point corresponds to the maximum number of pixels in the histogram of the given medical images. For instance, in **Fig. 2** (a), h(0) = 1943 is the peak point to be applied in embedding the secret message in the Lung CT image. In other words, the peak point of image's histogram will be a key factor of the hiding capacity. The higher peak point in the image, the larger the embedded capacity. In our scheme, we apply this characteristic to embed n bits in the medical image. The detail of data hiding scheme is described as follows.

Table 1. The comparison of 16-bit and 8-bit depth medical images

Medical Image Type	16-bit depth	8-bit depth
The Range of Intensity	65,536	256
Image Precision	High	Low
Duplicate Intensity	Less	More
Utilization Rate of Intensity	Low	High
Overflow Handling	Easy	Difficult
Underflow Handling	Easy	Difficult

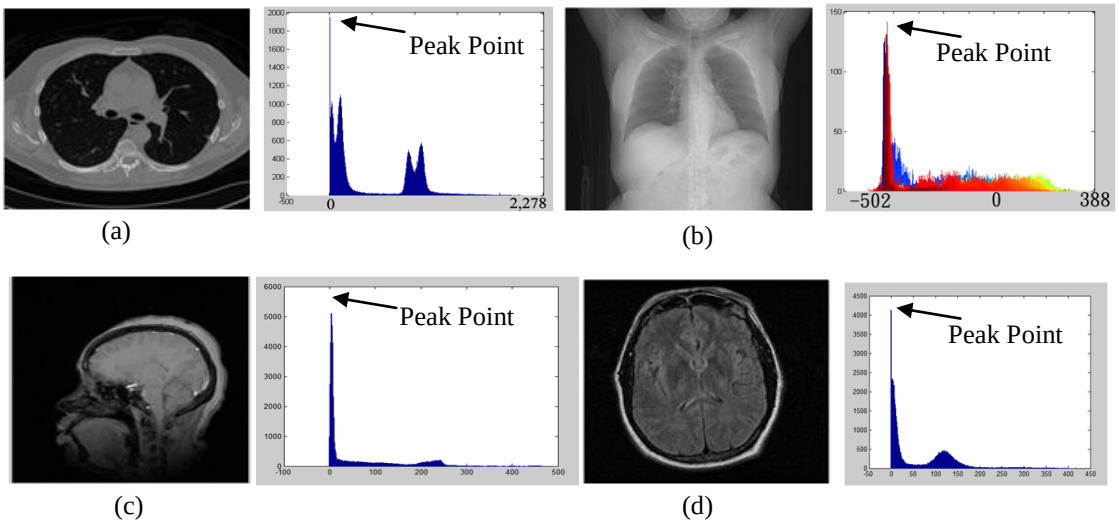

Fig. 2. Different kinds of medical images demonstrate distributions of intensities. (a) A Lung CT image with unsign 16- bit depth dcm format and histogram range from 0 to 2,342 (b) A Lung CT image with sign 16-bit depth dcm fromat and histogram range from -502 to 388 (c)(d) Brain MRI images with unsign 16-bit depth dcm format and histogram range from 0 to 436 , 0 to 417

2.1 Data Embedding

We apply pairs of (peak, zero) point in the image histogram and shift pixels histogram technique to embed secret bits. While the pixels of the intensity are shifted between the peak and zero points, an empty space will be created in the vicinity of the peak point. If the embedding bit is '1', its gray level will be increased by 1, otherwise it keeps intact. The peak and zero points need to be recorded because the image histogram will be changed. The detailed description for embedding secret bits will be demonstrated as shown in **Fig. 3**.

Step 1: Partition non-overlapping image blocks

Let I be an 16-bit depth gray scale medical image of size M × N. Image I will be partitioned into a set of $u \times v$ blocks. Therefore, the total number of blocks n_b can be computed as

$$n_b = \left\lfloor \frac{W}{u} \right\rfloor \times \left\lfloor \frac{H}{v} \right\rfloor \quad (1)$$

Where W is the image width, and H is the image height. The following steps 2-6 are repeated for each image block.

Step 2 : Select n as the parameter of Embedding Level (EL) in image block

EL is the number of (Peak, Zero) pairs preparing for embedding secret bits in an image block. After a pair ($Peak_i$, $Zero_i$) is selected, the embedding process will be performed. The embedding process includes empty peak histogram bins and embedding secret bits. Therefore, the embedding process will be performed EL times as shown in **Fig. 3** (d). EL will increase capacity largely, but the image quality is going to decrease.

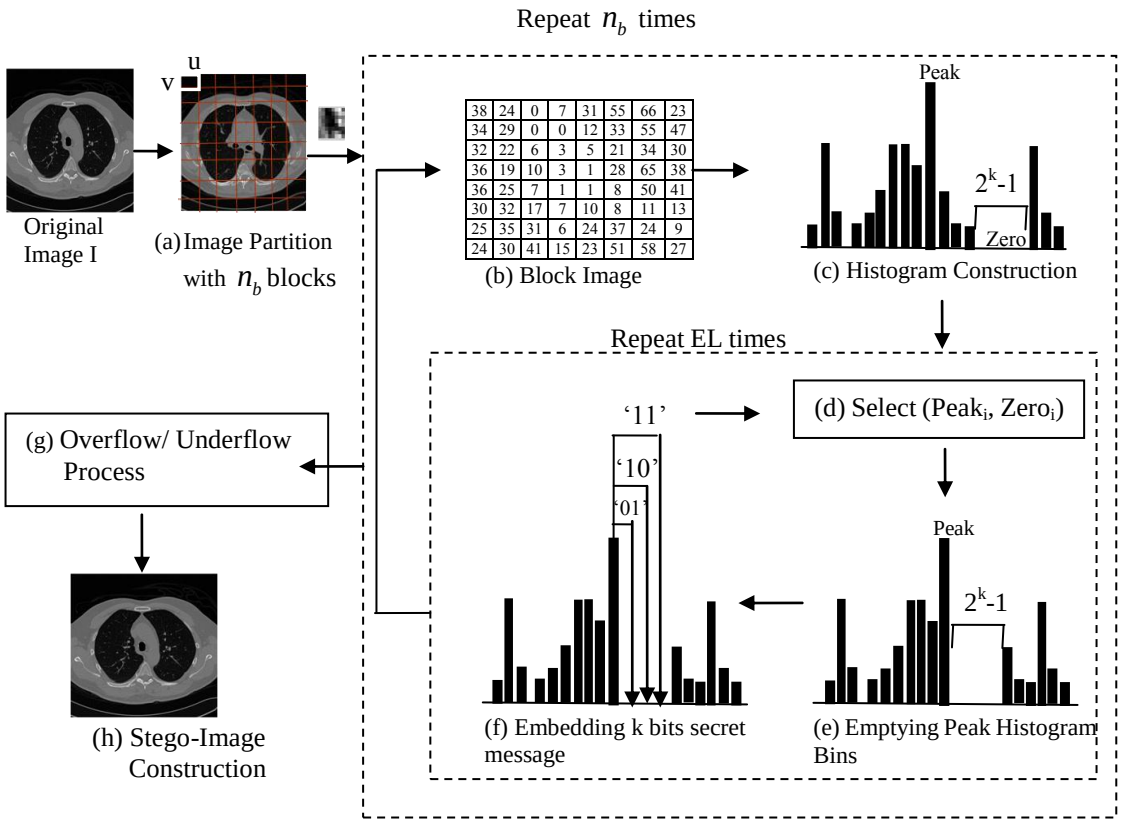

Fig. 3. The flowcharts of the data embedding with k = 2.

Step 3: Construct block histogram

An image block B(i, j) with u × v pixels are used to constructs a histogram demonstrated in **Fig. 3** (c). The maximum frequency is the peak point. And Zero points are the frequency 0. The following steps 4- 6 are repeated EL times.

Step 4 : Select pair of ($Peak_i$, $Zero_i$)

The peak point is maximum frequency in the image block. The strategy of zero point selection is searching 2^k-1 empty bins to embed k bits secret message nearest the peak point shown in **Fig. 4**. The zero point may be left side of Peak point or right side of Peak point. Because the distance between the peak and zero point will affect the image quality, the selection step is important step on the data hiding strategy. For instance, the PSNR of the pairs (0, 10) is better than PSNR of the pairs (0, 253). The pair of (0, 10) will change the gray values between 1 and 10. However, the pair of (0, 253) will change the gray values between 1 and

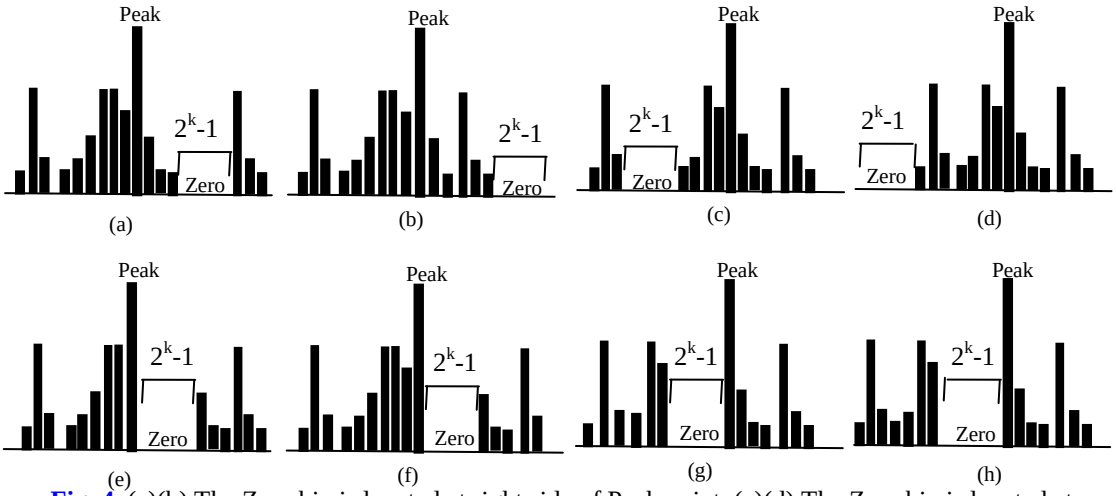

Fig. 4. (a)(b) The Zero bin is located at right side of Peak point. (c)(d) The Zero bin is located at left side of Peak point. After (a)(b)(c)(d) perform the empty bin operation, the histogram will be (e)(f)(g)(h).

253. The pair of ($Peak_i$, $Zero_i$) will be stored for being restored at extraction stage.

Step 5 : Empty histogram bins

The bins in range of [b_{Peak+1}, b_{Zero-1}] or [b_{Peak-1}, b_{Zero+1}] will be emptied with distance 2^k-1 to embed k bits. The formula is shown as follows.

$$H(i,j)=\begin{cases} H(i,j)+2^k-1 & if\ \ H(Zero\ )>H(Peak\ )\ \ and\ \ H(Peak\ )+1<H(i,j)<H(Zero\ )-1 \\ H(i,j)-2^k+1 & if\ \ H(Zero\ )<H(Peak\ )\ \ and\ \ H(Zero\ )+1<H(i,j)<H(Peak\ )-1 \end{cases} \quad (2)$$

Where k ≥ 0.

In case k = 2, the bins [b_{Peak+1}, b_{Zero-1}] are shifted rightward with distance 3 when Zero bin is located at right side of Peak point shown in **Fig. 4**(e)(f). On the contrary, [b_{Peak-1}, b_{Zero+1}] are shifted leftward with distance 3 when Zero bin is located at left side of Peak point shown in **Fig. 4**(g)(h). Therefore, this step will create 2^k-1 gaps at right (or left) side of the peak point.

Step 6 : Embed k bits secret message

The strategy of embedding message depends on two types : (1) Peak < Zero (2) Peak > Zero. The detail is described as follows.

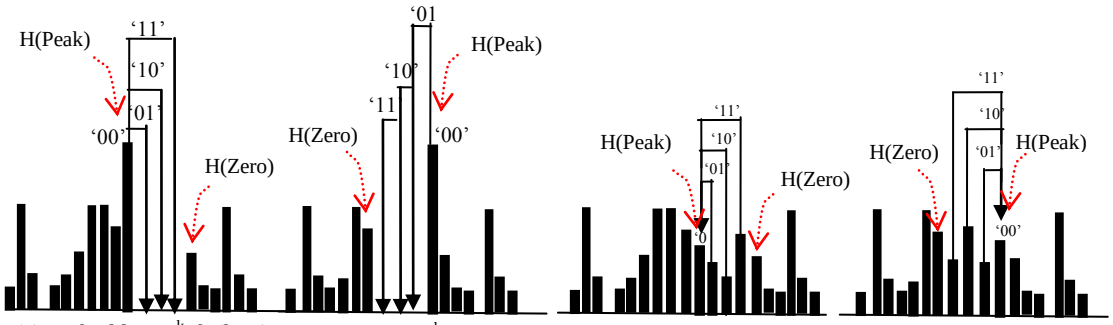

(a) Embedding $2^k \times k$ (k=2) bits i.e. 8 bits secret message in Type I

(b) Embedding $2^k \times k$ (k=2) bits secret message in Type II

(c) Extracting $2^k \times k$ (k=2) bits secret message in Type I

(d) Extracting $2^k \times k$ (k=2) bits secret message in Type II

Fig. 5. Embedding bit $2^k \times k$ (k = 2) in both Type I and Type II.

Type I. Peak < Zero

After performing empty histogram bins procedure, there are 2^k-1 empty bins located at right side of the peak point. We apply these bins to embed k bits secret message. The histogram will be modified in the following.

$$H'(Peak) = H(Peak) + w \quad (3)$$

Where w is the secret bits and $0 \le w < 2^k$. If k = 2, ther are four values (00, 01, 10, 11) can be embeded. If embedding bit is 00, the histogam of peak keeps intact. Otherwise, '01' '10' '11' will shift the histogram of Peak point rightward with distance 1, 2, and 3 respectively shown in **Fig. 5** (a).

Type II. Peak > Zero

There are 2k-1 empty bins will be created at left side of the peak point in subsequent the procedure of an empty peak histogram. The secret bits are embedded to 2k-1 empty bins. The histogram will be altered as follows :

$$H'(Peak) = H(Peak) - w \quad (4)$$

Where w is the secret bits and $0 \le w < 2^k$. The corresponding secret bits: '01' '10' '11' will shift the histogram of Peak point leftward with distance 1, 2, and 3 respectively. If the embedded data is '00', the histogram of Peak point will not be altered as shown in **Fig. 5** (b).

Step 7: Overflow/Underflow Processes

In high quality medical images, 16-bit depth is able to handle 65,536 discret levels of intensity. Let utilization rate of intensity be as follows.

$$\text{Utilization Rate of Intensity} = (\text{Max Intensity} - \text{Min Intensity}) / 2^{\text{bit-depth}} \quad (5)$$

Most of medical images have the low utilization rate. In other words, there are many empty discret levels of intensity in the high quality medical images. In order to handle overflow/underflow problems, we utilize these empty discret levels of intensity to solve

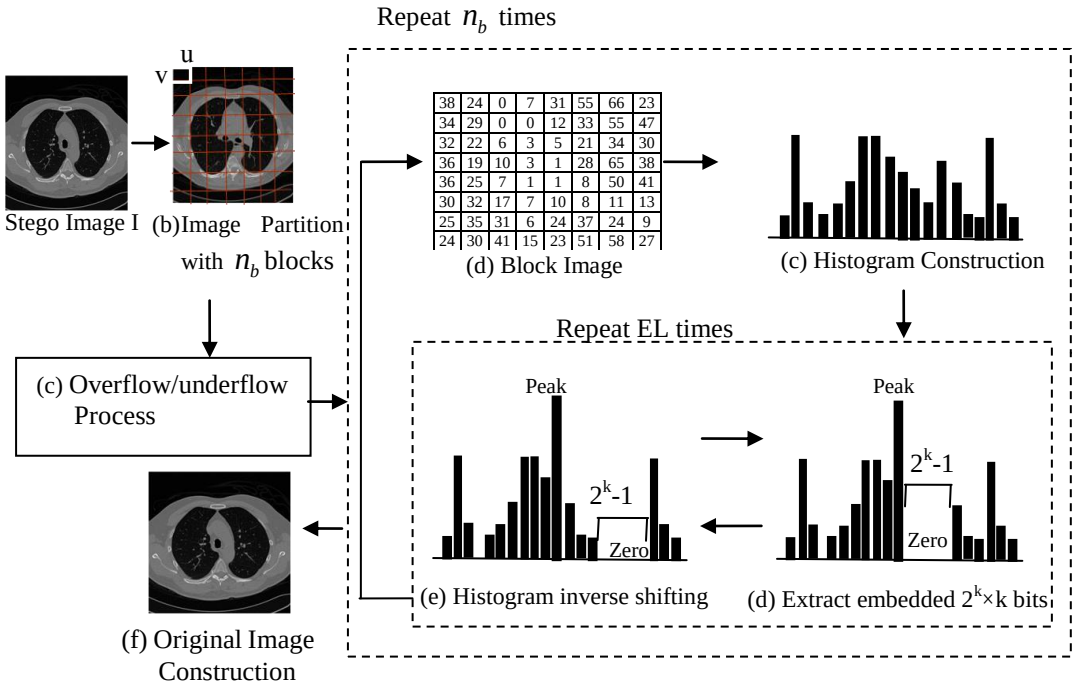

Fig. 6. The flowcharts of the data extraction with k = 2.

overflow/underflow. At first, we measure the hitogram concentrate and find empty bins $el = EL \times (2^k - 1)$ to shift a histogram as shown in **Fig. 7**.

Step 8: Stego-Image Construction

At this stage, the blockimages will be composed of a stego-imge as shown in **Fig. 3** (h).

2.2 Data Extraction

The data extraction will extract secret message correctly and restore the stego-image back to the original without any distortions with the details described below as shown in **Fig. 6**.

Step 1: Image partition

The stego-image will be partitioned into a set of $u \times v$ blocks.

Step 2: Overflow/Underflow process

According to the information of the shifting histogram from the embedding stage, we adjust the image histogram in order to restore the cover image correctly. The following steps 3-5 are repeatedly executed for each stego-image blocks.

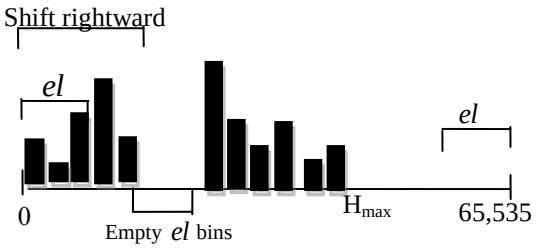

(d) In unsign 16-bit images, the process of underflow by shifting to rightward.

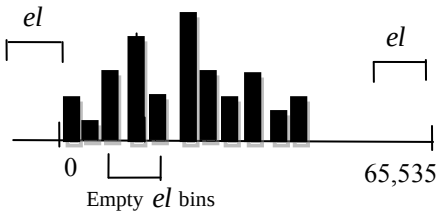

(e) After the underflow process in 16-bit unsign images.

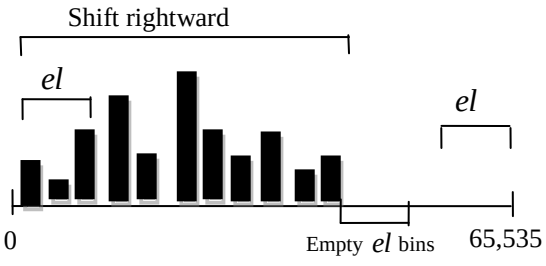

(c) In unsign 16-bit images, the empty bins are found in the rightmost of histogram.

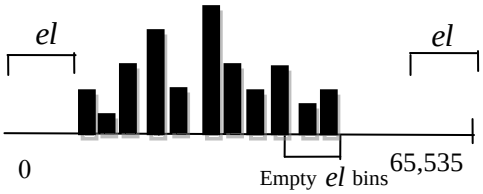

(b) After the underflow process in unsign 16-bit images.

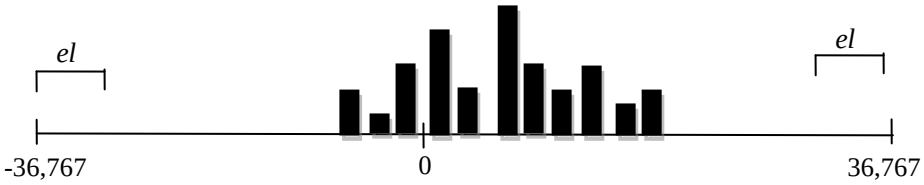

(a) In sign 16-bit images, few of underflow and overflow problem may occur.

Fig. 7. Overflow/Underflow Processing

Step 3: Construct histogram of a stego-image block

In this step, we apply each stego-image block to construct a histogram. The following steps 4-5 will be repeated EL times where EL is a parameter from an embedding process. In other words, EL is number of (Peak, Zero) points selected to be embedded secret bits.

Step 4: Extract embedded bits

A pair ($Peak_i$, $Zero_i$) is obtained by reversing the sequce of creating the information of pair ($Peak_i$, $Zero_i$) from an embedding process. There are two types of extracting secret messages: (1) Peak < Zero (2) Peak > Zero. The detailed is demonstrated as follows.

Type I. Peak < Zero

The gray values of the pixels in (Peak + $2^k - 1$) will be extracted as embedding bits $2^k \times k$. For instance, we embed 2 bits to each image block i.e. k = 2. Thus, there are four values (00, 01, 10, 11) extracted at bin of (Peak, Peak+1, Peak+2, Peak+3), respectively. The formula is demonstrated as follows.

$$w = \begin{cases} 00 & if \;\; H' = Peak \\ 01 & if \;\; H' = Peak + 1 \\ 10 & if \;\; H' = Peak + 2 \\ 11 & if \;\; H' = Peak + 3 \end{cases} \quad (6)$$

In other words, the pixel with gray value Peak indicates that the embedded data bit was 0. If the gray value of current pixel is equal to (Peak+1, Peak+2, Peak+3), it indicates the embedded data bit was (01, 10, 11), respectively. There a number of 2^2 bins of 2 bits (i.e. 8 bits) will be extracted.

Type II. Peak > Zero

The gray values of the pixels in (Peak - 2^k + 1) will be extracted as embedding bits $2^k \times k$. Assume we embed 2^2 (i.e. 00, 01, 10, 11) values of 2 bits to each image block, the embedding 8 bits can be extracted by the formula as follows.

$$w = \begin{cases} 00 & if \;\; H' = Peak \\ 01 & if \;\; H' = Peak - 1 \\ 10 & if \;\; H' = Peak - 2 \\ 11 & if \;\; H' = Peak - 3 \end{cases} \quad (7)$$

Therefore, the embedded data bit was extracted (00, 01, 10, 11) when the gray value of current pixel is equal to (Peak, Peak - 1, Peak - 2, Peak - 3) respectively.

Step 5: Histogram inverse shifting

After extracting secret bits, a histogram should be inversed by the transformation formula as shown in **Fig. 6**(d)(e).

$$H(i,j) = \begin{cases} H(i,j) - 2^k + 1 & if \;\; H(Zero) > H(Peak) \;\; and \;\; H(Peak) + 1 < H(i,j) < H(Zero) - 1 \\ H(i,j) + 2^k - 1 & if \;\; H(Zero) < H(Peak) \;\; and \;\; H(Zero) + 1 < H(i,j) < H(Peak) - 1 \end{cases} \quad (8)$$

Where H(Peak) and H(Zero) are from the information of the embedding stage.

Step 6: Original image construction

All extracted image blocks will be composed as original image demonstrated in **Fig. 6** (f).

3. Experimental Results

The proposed scheme was tested on many different kinds of high quality medical images (ex: CT, MRI, X-rays, SPECT) with DICOM (Digital Imaging and Communications in Medicine) from the National Cancer Imaging Archive [22]. Our method was implemented by MATLAB testing on Notebook with 2.67 GHz processor and 4.0 GB RAM. On average, the data hiding procedure required 46.12 seconds on a 512 × 512 CT slice and 256 × 256 MRI slice where block size < 2. Generally, the quality of stego-images was measured by PSNR (Peak Signal to Noise Ratio) and MSE (Mean Square Error). Therefore, the MSE is defined as follows.

$$\text{MSE} = \frac{1}{m \times n} \sum_{i=1}^{m} \sum_{j=1}^{n} (c_{ij} - \bar{c}_{ij})^2 \quad (9)$$

$$\text{PSNR} = 10 \times \log_{10} \frac{(Imaage\ bit\ depth)^2}{MSE} \quad (10)$$

Table 2. The results for 16-bit Grayscale CT Medical Image with different block sizes

Slice Number	Image size	Block Size	Capacity	bpp	PSNR	Time/sec
1.3.6.1.4.1.9328.50.3.6756.dcm	512 × 512	512 × 512	6,076	0.02	82.25	16.27
		256 × 256	7,296	0.03	81.70	10.69
		128 ×128	10,058	0.04	85.50	4.87
		16 ×16	28,902	0.11	87.41	20.34
		8 × 8	50,792	0.19	91.44	60.10
		8 × 4	71,542	0.27	94.42	113.85
		4× 8	72,042	0.28	94.28	119.06
		4 × 4	102,190	0.39	95.59	215.786
		2 × 2	274,352	1.05	92.21	935.64
		2 × 1	529,118	2.02	89.22	2,286.86
		1 ×2	528,970	2.02	89.24	2,274.30

Table 3. The results for 16-bit MRI mdeical Image on 000017.dcm

Slice Number	Image size	Block Size	Capacity	bpp	PSNR	Time / sec
1.3.6.1.4.1.9328.50.50.257784642039394959114962524759634087143\000001\000017.dcm	256 × 256	256 × 256	12,904	0.20	81.20	7.05
		128 ×128	12,936	0.20	81.26	4.79
		16 ×16	19,444	0.30	84.36	8.91
		8 × 8	25,722	0.39	85.43	18.60
		8 × 4	31,536	0.48	86.16	31.00
		4× 8	31,258	0.48	86.18	30.81
		4 × 4	40,014	0.61	87.47	53.72
		2 × 2	76,720	1.17	90.01	177.14
		2 × 1	136,150	2.08	89.01	366.38
		1 ×2	135,960	2.09	89.01	385.32

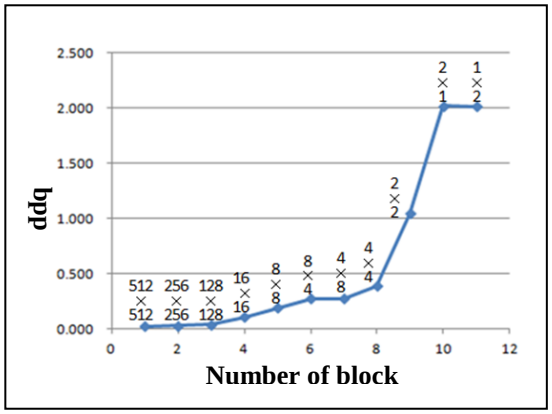

(a) The smaller image block size , the more bpp increases.

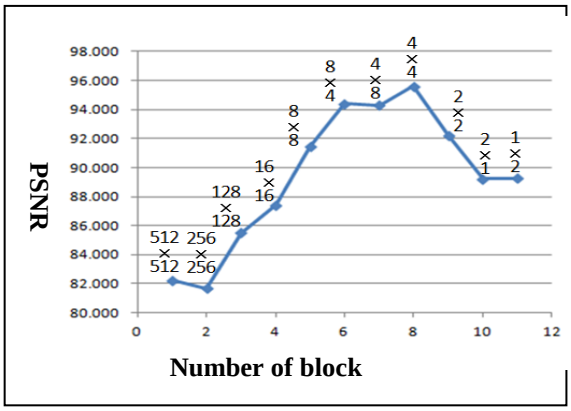

(b) In the image block size 4×4 has the highest PSNR.

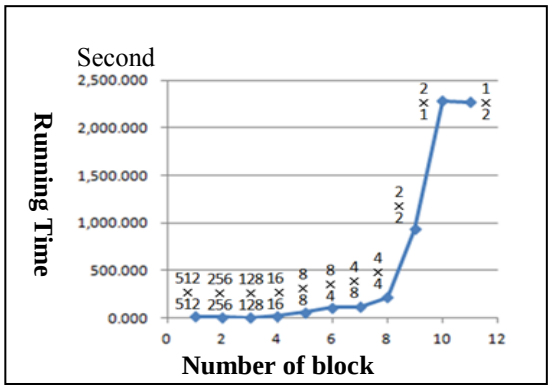

(c) The smaller image block size, the faster runing time.

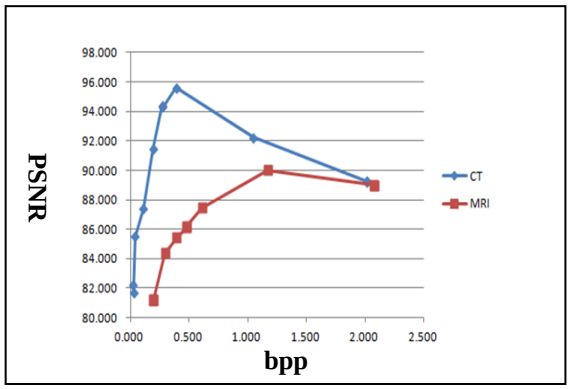

(d) The relation of PSNR and bpp on the CT and MRI image.

Fig. 8. The relation of bpp, PSBR, Running time and Block size

where an image bit depth adopted is 16. m and n are the width and height of the cover image and stego-image. c_{ij} *and* $\bar{c}_{ij}$ are intensities of the pixels located in cover and stego images respectively. The 16-bit depth CT and MRI medical images were tested with different block sizes shown in **Table 2** ~ **Table 3**. The smaller the block size, the more increase the capacity, as demonstrated as **Table 4**, **Table 5** and **Fig. 8** (a). And the running time of the scheme will increase when the image size becomes small. PSNR will be affacted by the distance of Zero Point and Peak Point because the shift histograms are perfermed in the embedding stage . In **Table 2**, the sample size 8 × 4 has the best PSNR value 94.42. The MRI image has the best PSNR value 90.01 in sample size 2 × 2 shown in **Table 3**. In **Fig. 8** (d), bpp is not an important factor to affect PSNR because the high capacity (bpp = 1.0) has still high PSNR in the case of CT (PSNR = 92) and MRI (PSNR = 90) image. The series of CT images are applied in our scheme as shown in **Table 5**.

4. Conclusion

Among patients and health care providers, reversible data hiding schemes are widely applied in the medical images systems. High quality images from modern medical devices are utilized to detect diseases or surgical treatment. Although most of reversible data hiding schemes experiments on 8-bit medical images, 16-bit depth CT and MRI medical images are still adopted as testing data. The 16-bit medical images have many advantages such as 65,536 discrete levels intensity, high image precision, and easy handling overflow/underflow problems. Due to low utilization rate of intensity in 16-bit depth, we apply empty histogram bins to solve overflow/underflow problems without salt-and-pepper. In our schemes, number of pairs (peak, zero) points are combined with the technique of shifting histogram to embed secret data. And the proposed method is suitable for 16-bit depth medical images as shown in the experimental results.

Table 4. The results for 16-bit MRI mdical Image on 000001.dcm

Slice Number	Image size	Block Size	Capacity	bpp	PSNR	Time /sec
1.3.6.1.4.1.9328.50.50.165429404613436780047444739484180811987\000000\000001.dcm	256 × 256	256 × 256	19,872	0.30	81.84	10.83
		128 ×128	19,880	0.30	81.93	7.24
		16 ×16	25,524	0.39	84.64	10.43
		8 × 8	32,108	0.49	85.39	20.86
		8 × 4	37,856	0.58	85.74	33.12
		4× 8	37,812	0.58	85.68	33.34
		4 × 4	46,608	0.71	86.07	57.05
		2 × 2	80,282	1.23	89.31	183.56
		2 × 1	135,908	2.07	89.74	382.75
		1 ×2	137,646	2.10	89.64	370.51

Table 5. The results for series of CT images

Slice Number	Image size	Block Size	Capacity	bpp	PSNR	Time /sec
1.3.6.1.4.1.9328.50.3.6322.dcm	512 × 512	2 × 2	275,970	1.05	92.13	922.94
1.3.6.1.4.1.9328.50.3.6328.dcm			275,568	1.05	92.23	924.34
1.3.6.1.4.1.9328.50.3.6332.dcm			275,786	1.05	92.30	893.25
1.3.6.1.4.1.9328.50.3.6336.dcm			275,638	1.05	92.28	907.87
1.3.6.1.4.1.9328.50.3.6496.dcm			275,402	1.05	92.26	924.58
1.3.6.1.4.1.9328.50.3.6500.dcm			275,674	1.05	92.16	952.37
1.3.6.1.4.1.9328.50.3.6504.dcm			275,662	1.05	92.09	972.10
1.3.6.1.4.1.9328.50.3.6508.dcm			275,946	1.05	92.02	925.17
1.3.6.1.4.1.9328.50.3.6512.dcm			275,656	1.05	92.04	952.37
1.3.6.1.4.1.9328.50.3.6516.dcm			275,444	1.05	92.05	904.11

Acknowledgements

We would like to thank National Cancer Institute for **providing** the CT image data used in this study.

References

[1] Chin-Chen Chang, Pei-Yan Pai, Chia-Ming Yeh, and Yung-Kuan Chan, "A high payload frequency-based reversible image hiding method," *Information Sciences*, vol. 180, pp. 2286-2298, 2010. Article (CrossRef Link)

[2] Chin-Chen Chang, Chih-Yang Lin, and Yi-Pei Hsieh, "Data hiding for vector quantizatin images using mixed-based notation and dissimilar patterns without loss of fidelity," *Information Sciences*, vol. 201, pp. 70-79, 2012. Article (CrossRef Link)

[3] Chin-Chen Chang, Chia-Chen Lin, Chun-Sen Tseng, Wei-Liang Tai, "Reversible hiding in DCT-based compressed images," *Information Sciences*, vol. 177, no. 13, pp. 2768-2786, 2007. Article (CrossRef Link)

[4] Chin-Chen Chang, Chih-Yang Lin, Yi-Hsuan Fan, "Lossless data hiding for color images based on block truncation coding," *Pattern Recognition*, vol. 41, pp.2347-2357, 2008. Article (CrossRef Link)

[5] Chia-Chun Wu, Shang-Juh Kao, and Min-Shiang Hwang, "A high quality image sharing with steganography and adaptive authentication scheme," *The Journal of Systems and Software*, vol. 84, pp. 2196-2207, 2011. Article (CrossRef Link)

[6] Chia-Chun Wu, Min-Shiang Hwang, and Shang-Juh Kao, "A new approach to the secret image sharing with steganography and authentication," *The Imaging Science Journal*, vol. 57, no. 3, pp. 140-151, 2009. Article (CrossRef Link)

[7] S-F Chiou, I-En Liao, and Min-Shiang Hwang, "A capacity-enhanced reversible data hiding scheme based SMVQ," *The Imaging Science Journal*, vol. 59, pp. 17-24, 2011. Article (CrossRef Link)

[8] Zhiguo Chang and Jian Xu, "Reversible run length data embedding for medical images," Communication Software and Networks (ICCSN), in *Proc. of 2011 IEEE 3rd International Conference*, pp. 260-263, 2011.

[9] M. Fallahpour, D. Megias, and M. Ghanbari, "Reversible and high-capacity data hiding in medical images," *IET Image Processing*, vol.5, Iss. 2, pp. 190-197, 2011. Article (CrossRef Link)

[10] Min-Shiang Hwang, K. F. Hwang, and Chin-Chen Chang, "A timestamping protocol for digital watermarking," *Applied Mathematics and Computation*, vol. 169, pp. 1276-1284, 2005. Article (CrossRef Link)

[11] Li-Chin Huang, Lin-Yu Tseng, and Min-Shiang Hwang, "The study of data hiding in medical image," *International Journal of Network Secuity*, vol. 14, no. 5, pp. 243-251, 2012.

[12] Li-Chin Huang, Lin-Yu Tseng, and Min-Shiang Hwang, "A reversible data hiding method by histogram shifting in high quality medical images," *Journal of Systems and Software*, Available online 3 December, 2012. Article (CrossRef Link)

[13] H. -J. Kim, V. Sachnev, Y. Q. Shi, J. Nam, and H. -G. Choo, "A novel difference expansion transform for reversible data embedding," *IEEE Transactions on Information Forensics and Security*, vol. 3, no. 3, pp. 456-465, Sep. 2008. Article (CrossRef Link)

[14] B. Karthikeyan, S. Ramakrishnan, V. Vaithiyanathan, S. Sruti, and M. Gomathymeenakshi, "An Improved Steganographic Technique Using LSB Replacement on a Scanned Path Image," *International Journal of Network Security*, vol.15, no.1, pp.314-318, 2013.

[15] Der-Chyuan Lou, Ming-Chiang Hu, and Jiang-Lung Liu, "Multiple layer data hding scheme for medical images," *Computer Standards and Interfaces*, vol. 31, pp.329-335, 2009. Article (CrossRef Link)

[16] Hao Luo, Fa-Xin Yu, Hua Chen, Zheng-Liang Huang, Hui Li, and Ping-Hui Wang, "Reversible data hiding based on block median preservation," *Information Sciences*, vol. 181, pp.308-328, 2011. Article (CrossRef Link)

[17] Zhichen Ni, Yun Q. Shi, Nirwan Ansari, Wei Su, Qibin Sun and Xiao Lin, "Robust lossless image data hiding designed for seim-fragile image authentication," *IEEE Transactions on Circuits and Systems for Video Technology*, vol. 18, pp.497-509, 2008. Article (CrossRef Link)

[18] Z.M. Lu., J.X. Wang, B.B. Liu, "An improved lossless data hiding scheme based on image VQ-index residual value coding," *The Journal of Systems and Software*, vol. 82, no. 6, pp.1016-1024, 2009. Article (CrossRef Link)

[19] Zhensong Liao, Yan Huang, and Chisong Li, "Research on Data Hiding Capacity," *International Journal of Network Security*, vol.5, no.2, pp.140–144, 2007.

[20] Z. Ni, Y, -Q. Shi, N. Ansari, and W. Su, "Reversible data hiding," *IEEE Transactions on Circuits and Systems for Video Technology*, vol. 16, pp. 354-362, 2006. Article (CrossRef Link)

[21] Zhichen Ni, Yun Q. Shi, Nirwan Ansari, Wei Su, Qibin Sun and Xiao Lin, "Robust lossless image data hiding designed for seim-fragile image authentication," *IEEE Transactions on Circuits and Systems for Video Technology*, vol. 18, pp.497-509, 2008. Article (CrossRef Link)

[22] National Cancer Imaging Archive. Available at https://imaging.nci.nih.gov/.

[23] Palak K. Amin, Ning Liu, and K. P. Subbalakshmi, "Statistical Attack Resilient Data Hiding," *International Journal of Network Security*, vol.5, no.1, pp.112–120, 2007.

[24] Mrigank Rochan, Santosh Hariharan, and Kumar Rajamani, "Data hiding scheme for medical images using lossless code for mobile HIMS," in Proc. of Third International Conference on Communication Systems and Networks, pp. 1-4, 2011.

[25] S. S. Sujatha and M. Mohamed Sathik, "A novel DWT based blind watermarking for image authentication," *International Journal of Network Security*, vol. 14, no. 4, pp. 223-228, 2012.

[26] Yun Q. Shi, Zhicheng Ni, Dekun Zou, Changuin Liang and Guourong Xuan, "Data hiding fundamentals, algorithms and applications," *Circuits and Systems*, 2004 IEEE International Symposium, pp. 33-36, 2004.

[27] D. B. Satre and R. V. Pawar, "Preserve robustness for image data hiding," in *Proc. of Second International Conference on Computer Research and Development*, pp. 707-711, 2010. Article (CrossRef Link)

[28] J. Tian, "Reversible data embedding using a difference expansion," *IEEE Transactions on Circuits and Systems for Video Technology*, vol. 13, no 8, pp. 890-896, Aug. 2003. Article (CrossRef Link)

[29] S. Maria Celestin Vigila and K. Muneeswaran, "Nonce based elliptic curve cryptosystem for text and image applications," *International Journal of Network Security*, vol. 14, no. 4, pp. 236-242, 2012.

[30] Christophe De Vleeschouwer, Jean-Francois Deloaigle, and Benoit Macq, "Circular interpretation of bijective transformation in lossless watermarking for media asset management," *IEEE Transactions on Multimedia*, vol. 5, pp. 97-104, 2003. Article (CrossRef Link)

[31] Nan-I Wu and Min-Shiang Hwang, "Data hiding: Current status and key issues" *International Journal of Network Security*, vol. 4, no. 1, pp. 1-9, Jan. 2007.

[32] Nan-I Wu, Chung-Ming Wang, Chwei-Shyong Tsai, and Min-Shiang Hwang, "A certificate-based watermaking scheme for coloured images," *The Images Science Journal*, vol. 56, pp. 326-332, 2008.

[33] Wei-Jen Wang, Cheng-Ta Huang, and Shiuh-Jeng Wang, "VQ applications in steganorgraphic data hiding upon multimedia images," *IEEE Systems Journal*, vol. 5, no. 4, pp. 528-537, 2011. Article (CrossRef Link)

[34] Chi-Yao Weng, Shiuh-Jeng Wang, Jonathan Liu, and Dushyant Goyal, "Prediciton-based reversible data hiding using empirical histograms in images," *Transactions on Internet and Information Systems*, vol. 6, no. 4, pp. 1248-1266, 2012. Article (CrossRef Link)

[35] Chung-Ming Wang, Nan-I Wu, Chwei-Shyong Tsai and Min-Shiang Hwang, "A high quality steganographic method with pixel-value differencing and modulus function", *The Journal of Systems and Software*, vol. 81, Iss. 1, pp. 150-158, 2008.

[36] Shangping Zhong, Xueqi Cheng, and Tierui Chen, "Data Hiding in a Kind of PDF Texts for Secret Communication," *International Journal of Network Security*, vol.4, no.1, pp.17–26, 2007.

Li-Chin Hwang received the B.S. and M.S. in Information Management from Chaoyang University of Technology (CYUT), Taichung, Taiwan, in 2001 and in 2003. She is currently working toward the PhD degree in the Department of Computer Science and Engineering at the National Chung Hsing University (NCTU), Taiwan. Her current research interests include information security, cryptography, medical image, and mobile communications.

Min-Shiang Hwang received the B.S. in Electronic Engineering from National Taipei Institute of Technology, Taipei, Taiwan, ROC, in 1980; the M.S. in Industrial Engineering from National Tsing Hua University, Taiwan, in 1988; and the Ph.D. in Computer and Information Science from National Chiao Tung University, Taiwan, in 1995. He also studied Applied Mathematics at National Cheng Kung University, Taiwan, from 1984-1986. Dr. Hwang passed the National Higher Examination in field "Electronic Engineer" in 1988. He also passed the National Telecommunication Special Examination in field "Information Engineering", qualified as advanced technician the first class in 1990. He was a chairman of the Department of Information Management, Chaoyang University of Technology (CYUT), Taiwan, during 1999-2002. He is currently a professor of the department of Management Information System, National Chung Hsing University, Taiwan, ROC. He obtained 1997, 1998, 1999, 2000, and 2001 Outstanding Research Awards of the National Science Council of the Republic of China. He is a member of IEEE, ACM, and Chinese Information Security Association. His current research interests include electronic commerce, database and data security, cryptography, image compression, and mobile computing. Dr. Hwang had published 170+ articles on the above research fields in international journals.

Lin-Yu Tseng received the B.S. degree in mathematics from the National Taiwan University, in 1975, the M.S. degree in computer science from the National Chiao Tung University, Taiwan, in 1978, and the Ph.D. degree in computer science from National Tsing Hua University, Taiwan, in 1988. He is presently a Professor in the Department of Computer Science and Communication Engineering, Providence University, Taiwan. His research interests include evolutionary computation, neural network, multimedia systems, image processing, pattern recognition, and bioinformatics.